

Reliability Improvement Techniques for Spot Weld of High Tensile Strength Steel Sheets for Automobiles

Chisato WAKABAYASHI* Yasunobu MIYAZAKI
Seiji FURUSAKO Fuminori WATANABE

Abstract

The use of high tensile strength steel sheets for automobiles is increasing to achieve high crashworthiness and high environmental performance. The history of high tensile strength steel sheets and the problems of spot weld with such steel sheets were introduced. A major problem is the decrease in the weld strength which prevents expansion of the use of high tensile strength steel sheets. To solve this problem, we developed some spot welding techniques which improve the scattering of weld strength.

1. Introduction

Demand for high environmental performance and safety performance of automobiles is growing. In Japan, the fuel consumption target of 20.3 km/L in fiscal 2020, a 24.1% improvement from the 16.3 km/L in fiscal 2009, has been set for environmental performance.¹⁾ Also in other countries like the EU, USA and China, control values and target values are set respectively in a similar move. Furthermore, the UK and France decided recently to abolish totally the sales of diesel and gasoline engine cars not later than 2040.

Regarding safety performance, the revision of regulations and safety-performance assessment items is scheduled, and improvement in car safety performance is essential. To improve environmental performance, reduction in car body weight is effective. Meanwhile, increasing car body weight is effective for enhancing collision safety performance. Accordingly, for compatibility of contradictory factors, various developments are necessary, among which material development plays an important role. High tensile strength steel that can exert strength with lighter weight has been developed, and the application of high tensile strength steel sheets is expanding. Hereafter, the increase in the tensile strength of steel sheets is expected to continue.

Steel sheets used for car body structure are press-formed and formed into parts by resistance spot-welding. The strength of the weld joint of spot resistance welding of high tensile strength steel sheets does not always increase jointly with the increase in the strength of steel sheets. A phenomenon of conversely decreasing strength in a separation mode is reported.²⁾ When a collision takes place, unless the weld joint strength is secured, the performance ex-

pected for the parts cannot be fully exerted, and high strength cannot be achieved. Therefore, enhancement of weld joint strength in the resistance spot welding of high tensile strength steel sheets is essential, and research and development have been promoted along with expansion of the application of high tensile strength steel sheets.

For example, conventional methods include enlarging the nugget diameter and/or tempering of the welded part by tempering the current.³⁾ In addition, segregation-alleviating post-heat current application has been developed.⁴⁻⁶⁾ This report introduces techniques of improving weld joint strength by the Heat Affected Zone (hereafter HAZ) autotempering-promoting post-heat current application that is capable of improving toughness of the HAZ⁷⁾ and segregation-alleviating post-heat current application. Furthermore, from the viewpoint of improving the reliability of weld joint strength, it is necessary to reduce its scattering. Then, the relationship between post-heat current introduced as a means for improving weld-joint strength and the scattering of weld strength is also discussed.

2. High Tensile Strength Steel Sheets Used for Automobiles

The tensile strength of steel used for automobiles ranges from 270 MPa to about 4000 MPa class, and the highest strength is that of the steel chord used for automobile tires. As for structural member material, cold-rolled steel sheets of 1180 MPa class and 1470 MPa class steel sheets for hot-stamping usage have been developed and practically applied. Enhancing the tensile strength of steel deteriorates formability (ductility, local deformability, etc.), and the development of steel has been conducted aiming at establishing the com-

* Senior Researcher, Dr. Eng., Welding & Joining Research Lab., Steel Research Laboratories
20-1 Shintomi, Futtsu City, Chiba Pref. 293-8511

patibility of both factors. Among them, Dual Phase (hereinafter referred to as DP) steel and Transformation Induced Plasticity (hereinafter referred to as TRIP) steel are representative. Triggered by the Oil Crisis⁸⁾, research and development of DP steel was extensively conducted to meet the requirement of improving fuel consumption.

As a result thereof, high tensile strength DP steel sheets having a tensile strength higher than 590 MPa class provided with high press-formability that cannot be achieved by solute strengthening or precipitation strengthening alone are now practically used in a wide range of fields. In the DP steel, in the case that ductility is prioritized, the dual phase microstructure contains ferrite and martensite, and in the case that hole expandability is prioritized, the microstructure contains bainite. Practical application of 980 MPa and 1180 MPa class is also now in progress. Low alloy TRIP steel aimed at higher ductility has been developed extensively. The TRIP phenomenon was reported by Zackay in 1967⁹⁾.

However, as the addition of a large quantity of Ni and Mn to stabilize austenite was required at first to retain austenite in steel sheets, practical application did not progress because of the high cost. However, later on, low alloy TRIP steel that stabilizes austenite with carbon was developed, and a 780 MPa class hot-rolled steel sheet was employed for actual parts in 1989. Currently, extensive research and development over the low alloy TRIP steel are continuously conducted. In addition, to avoid the problems of poor cold press formability, increase in pressing load and insufficient shape-freezing property, hot-stamping steel sheets are also used, in which the steel sheet is heated up to the austenite region, simultaneously press-formed and quenched. In all high tensile strength steel sheets, the contents of C, Si and Mn tend to increase characteristically as compared with mild steel and 440 MPa class steel sheets.

3. Problems Pertaining to Resistance Spot Welding of High Tensile Strength Steel Sheets

3.1 Outline of weldability in resistance spot welding of high tensile strength steel sheets

In high tensile strength steel sheets, when two sheets are pinched with electrodes, the contact of the two sheets is poor as compared with that of mild steel sheets. Therefore, the contact area diameter is smaller, and the current path fails to widen. This phenomenon is particularly remarkable when there is a gap between the sheets. Furthermore, spattering tends to occur as the resistance value is high, which means that it is difficult to define the optimum range of current that ensures an appropriate nugget diameter. Accordingly, countermeasures such as high pressing force, elongation of current application time, and/or alteration of current application conditions are occasionally required.

3.2 Weld joint strength in resistance spot welding of high tensile strength steel sheets

As described earlier, in separation mode, sometimes the weld joint strength of high tensile strength steel sheets does not increase, and conversely decreases instead even when the steel sheet strength is increased. Tensile Shear Strength (hereinafter referred to as TSS) and Cross Tensile Strength (hereinafter referred to as CTS) are widely used as indexes for evaluating weld joint strength of spot welding. The latter CTS is used to represent the weld joint strength in separation mode. There is a report that CTS does not increase, and rather decreases instead in high tensile strength steel sheets, particularly in steel sheets of 780 MPa class or above.²⁾ This phenomenon significantly impedes the expansion of application of high tensile strength steel sheets. Hardened and embrittled nuggets are also

considered to deteriorate the weld joint strength of high tensile strength steel sheets.⁴⁾

In many cases of high tensile strength steel, nuggets and HAZ become martensitic. Particularly when the carbon content is high, as hardness increases,¹⁰⁾ they tend to become more brittle. With a nugget so brittle, or of low toughness microstructure, plug fracture does not occur and cracks propagate in the nugget instead, and partial plug fracture and/or matrix fracture occurs. The transition in the fracture morphology causes the deterioration of weld joint strength. In the past, focus was placed on the influence of steel compositions on the fracture morphology, the criteria of optimum steel compositions as to whether plug fracture takes place was determined by the boundary, and the compositions thus obtained were formulated and called carbon equivalent (hereinafter referred to as C_{eq}). It is reported that, by controlling C_{eq} to below a certain limit, plug fracture can be secured.¹¹⁾ The development of steel sheets is conducted by setting composition criteria using C_{eq} . However, for the development of further sophisticated high tensile strength steel sheets, occasionally steel compositions that exceed the criteria have to be employed. For the welding of such steel sheets, it is necessary to improve the reliability of spot weld joint by further developing the spot welding method.

4. Method for Improving Weld Joint Strength in Resistance Spot Welding of High Tensile Strength Steel Sheets

Spot-weld joint strength runs short occasionally in high functional steel sheets such as steel sheets equipped with high tensile strength and excellent formability, and steel for hot stamping. Regarding this problem, technologies developed to date are introduced together with experimental results and examination thereon.

4.1 Experiment and result thereof pertaining to improvement in weld joint strength

4.1.1 Experiment

Two types of steel processed through melting, rolling and annealing in a laboratory were used. The sheet thickness is 1.2 mm, and C_{eq} , C and P contents of these steels are shown in Table 1. C_{eq} of the following formula was used.¹²⁾

$$C_{eq} = C + 1/6Mn + 1/5(Cr+Mo+V) + 1/15(Ni+Cr) \quad (1)$$

They are termed as Steel A and Steel B hereinafter. Two sheets of identical steel were joined face to face and welded. A servomotor-pressurizing type single phase AC spot welding machine (power frequency 50 Hz) was used. Current was applied in two steps as schematically shown in Fig. 1, wherein the first step current (I_1) was applied to form a nugget (hereinafter referred to as the main current) and the second step current (I_2) was the post-heat current to reform the metallic structure of the nugget (molten and then solidified part) and HAZ. In the experiment, the second current (post-heat current) application time varied in the range of 0–1.4 s. The main current I_1 was adjusted so as to obtain a nugget diameter of $5\sqrt{t}$ ($=5.5$ mm, t : sheet thickness) and the post-heat current I_2 was set at 95% of the main current. In addition, the cooling time was fixed at 0.04 s. The optimum conditions of the cooling time and the post-heat current

Table 1 Chemical compositions of samples (mass%)

	C	Mn	P	C_{eq}
Steel A	0.20	1.3	0.020	0.41
Steel B	0.21	2.9	0.010	0.69

vary depending on sheet thickness and the specific resistance of the steel sheet.

Furusako et al. reported the result of their study by means of heat conduction analysis under post-heat current application conditions intended to alleviate the segregation at the nugget edge,¹³⁾ and the result was referred to as a guide to determine the cooling time and the post-heat current value. Post-heat current application time exceeding the range recommended by Furusako et al. was also taken into consideration in the experiment as the experiment was conducted to reform HAZ in addition to segregation alleviation.

Cross tensile strength test specimens were prepared under the abovementioned welding conditions (n=3), and the tensile strength test was conducted at a tension rate of 10 mm/min and CTS was measured. Afterwards, the fractured sample section surface was observed by an optical microscope, and furthermore, observation and analysis of the microstructure of the weld part were conducted by Scanning Electron Microscope (hereinafter referred to as SEM) and Electron Backscatter Diffraction (EBSD). Element mapping was conducted by means of Field Emission-Electron Probe Micro Anal-

ysis (hereinafter referred to as FE-EPMA).

4.1.2 CTS and fractured sample surface after CTS test

The two steels shown in Table 1 were welded with varied post-heat current application time and CTS was measured, the result of which is shown in Fig. 2 (mean value of n=3 is plotted). In Steel A, CTS increases with relatively short post-heat current application time. While in Steel B, CTS gradually increases up to about 0.6s of post-heat current application time and becomes saturated thereafter.

Figure 3 shows the cross section images of the samples after the CTS test without and with post-heat current application. On the section of the sample without post-heat current application, propagation of cracks into a nugget is observable at the sections shown by broken line circles. However, on the samples with a post-heat current application time of 0.1 s and/or 0.6 s, such propagation of cracks into a nugget is not observable. This effect, which will be shown in detail in a later section, is considered to be attributed to the alleviated segregation at the edge of the nugget.^{3,4)} As for Steel B, as shown in Fig. 4, without post-heat current application, cracks propagate into the nugget (shown with broken line circles) similarly to Steel A, which is suppressed by a post-heat current of 0.1 s.

However, HAZ of the sample of Steel B that is provided with a post-heat current application of 0.1 s does not show any noticeable

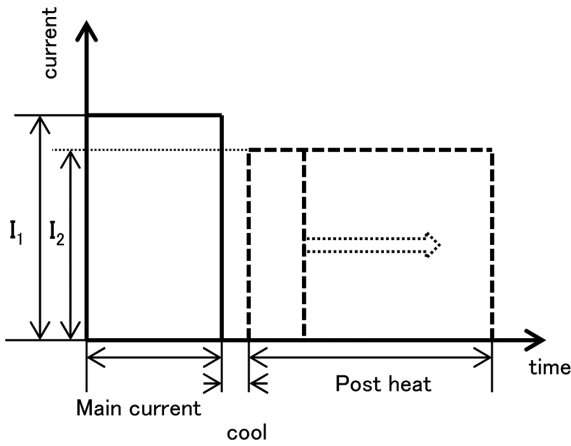


Fig. 1 Schematic image of current pattern

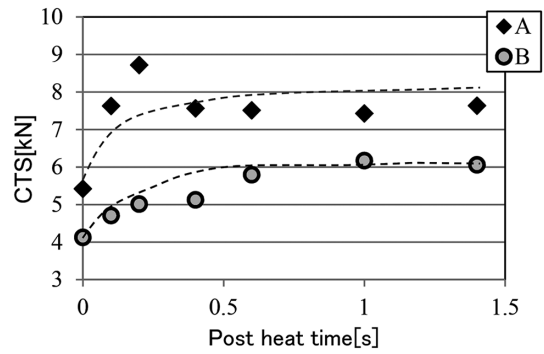
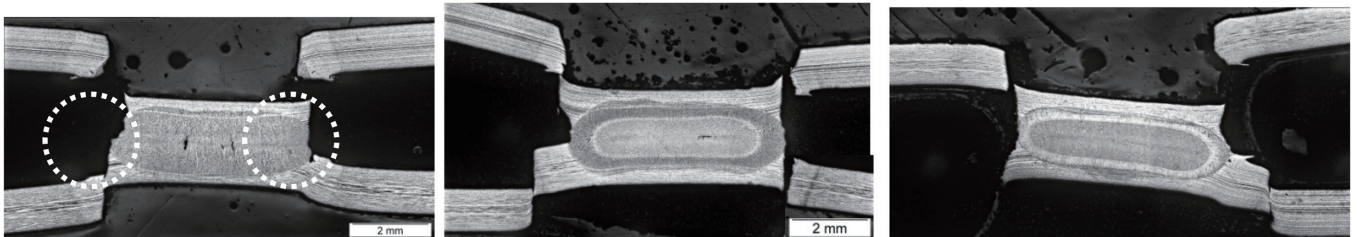


Fig. 2 Post heat time and CTS

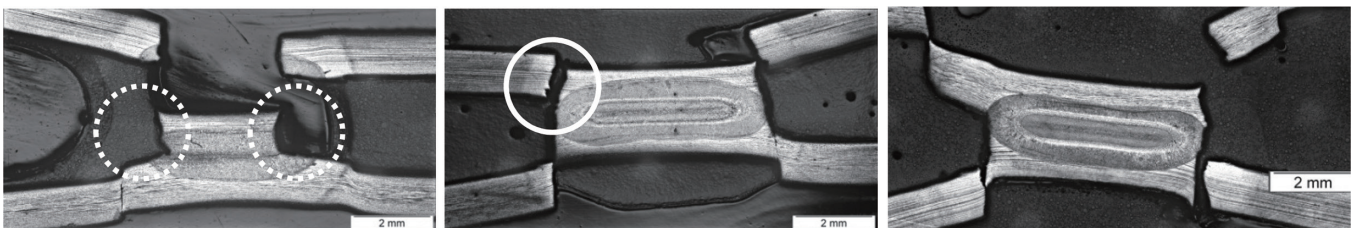


Without post heat

Post heat 0.1s

Post heat 0.6s

Fig. 3 Cross section image (steel A)



Without post heat

Post heat 0.1s

Post heat 0.6s

Fig. 4 Cross section image (steel B)

deformation, and does not appear fractured in the ductility mode (Fig. 4, shown with a solid line circle). On the other hand, in the sample that is provided with a post-heat current application of 0.6 s, either of the fractured section accompanies noticeable deformation and shows fracture in the ductility mode. The transition in fracture morphology is considered to increase weld joint strength. Details of the phenomena caused by post-heat current application are shown hereunder.

4.2 Improvement in CTS by controlling fracture of nugget by means of segregation alleviation

The propagation of cracks within a nugget could be prevented with a short post-heat current application time in both Steel A and Steel B. This phenomenon was proposed a few years ago, and was considered to be attributed to the increase in toughness realized by the alleviation of solidification segregation at the nugget edge.^{4-6,7,13)} Segregation is considered to be alleviated in the following manner: after application of the main current, the nugget edge is solidified during cooling (no current application), which is reheated by the subsequent application of post-heat current, and the segregated elements are dissipated thereby.

To ascertain the effect, the nugget edge of Steel A was observed by EPMA, the result of which is shown in Fig. 5. Figure 5 is a mapping of phosphorus (hereinafter referred to as P), an embrittling element. In the case without post-heat current application, remarkable segregation is observed within the nugget (above left of the broken line), which originated in solidification. In the sample with a post-heat current application of 0.1 s, segregation within the nugget appears slightly alleviated as compared with the sample with single current application. In addition, in the sample with a post-heat current application of 0.6 s, the segregation is alleviated to the extent that segregation becomes almost unrecognizable in the EPMA image. Steel B also showed a similar trend.

When an embrittling element such as P is locally segregated, toughness of the part deteriorates. However, the local segregation is alleviated by means of post-heat current application, and toughness is improved. In this experiment, Fig. 5 shows that the longer the post-heat current application time, the more the segregation tends to be alleviated. However, both in Steel A and Steel B, 0.1 s is sufficient to prevent the propagation of cracks in a nugget. Diffusion of atoms within 0.1 s is verified with a focus on P. Figure 6 shows the temperature histories at the position 100 μm inside from the edge, estimated by means of thermo-elastic plasticity analysis. The case with main current application only (broken line) and the case with

post-heat current application (solid line) are shown. When the post-heat current application of 0.1 s is provided, the edge is heated up to almost 1400°C after being cooled to about 1200°C. During the post-heat current application, diffusion distance x is sought based on the following assumption: temperature is constant at 1300°C, diffusion coefficient = D , content gradient is disregarded, $x = \sqrt{Dt}$, and $D = D_0 \exp(-Q/RT)$ (frequency term $D_0 = 8.7[10^{-4} \text{m}^2/\text{s}]$, activation energy $Q = 273[10^3 \text{J/mol}]$, R : gas constant, T : temperature). As a result, x of 0.4 μm is obtained.

Furusako et al.¹²⁾ reported that the width of the solidification segregation with only the main current application is 1–5 μm, and recommend that the segregation should be diffused more than 0.2 μm in post-heat current application. The diffusion distance estimated with the calculation result of temperature histories is 0.4 μm, and this satisfies the value sufficiently. Accordingly, the effect of segregation alleviation is obtained with the post-heat current application of 0.1 s, and in both Steel A and Steel B, propagation of cracks into a nugget could be suppressed. In addition, for Steel A, as CTS is sufficiently improved by the segregation alleviation at the nugget edge with the post-heat current application of about 0.1 s, a longer post-heat current application is unnecessary.

Next, the mechanism of improving CTS by means of post-heat current application longer than 0.1 s is introduced.

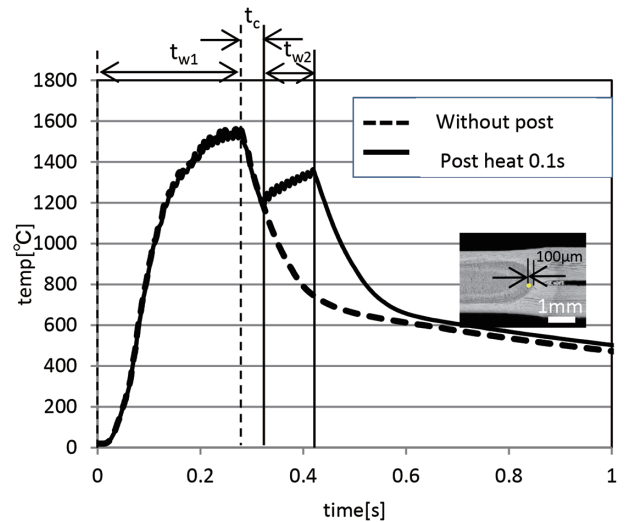


Fig. 6 Estimated temperature histories of nugget edge

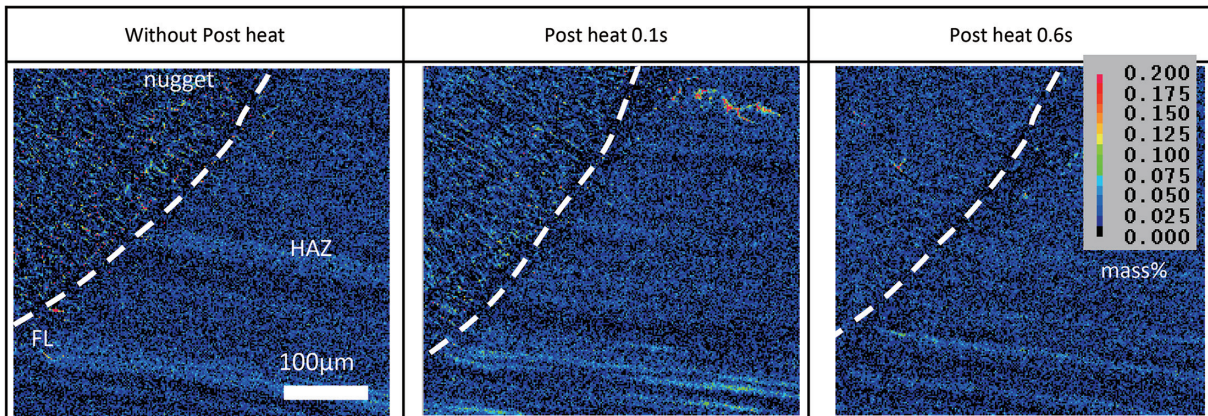


Fig. 5 EPMA mapping (P) of the edge part (steel A)

4.3 Improving toughness of fractured part by promoting HAZ autotempering

4.3.1 Reforming of microstructure of HAZ by increasing post-heat current application time

In Steel B, HAZ exhibits fracture in the ductility mode when relatively long post-heat current is applied, and CTS increases against segregation alleviating post-heat current application (post-heat current application time is 0.1 s). The reason for this is as follows. As the fracture morphology has changed, HAZ microstructure was considered to have also been reformed, and observation by SEM was conducted, the result of which is shown in Fig. 7. The observation point was set at the position 100 μm apart from the nugget edge and 200 μm apart from the sheet joining surface. Both Steel A and Steel B exhibited lath martensite microstructure.

In Steel A, under all conditions, regions containing fine precipitates are recognized. In Steel B, although such precipitates are recognized under the conditions of with 0.6 s of post-heat current application, precipitates are not recognized under the conditions of without post-heat current application and with 0.1 s of post-heat current application. These precipitates are carbides of the ferrous family and exhibit microstructures similar to those of cementite. Furthermore, these precipitates are not observed in the microstructures when post-heat current is not applied. Therefore, they are not the residue of carbide of the once molten base metal, but that produced during the welding process. Figure 8 shows the temperature histories estimated by means of thermo-elastic plasticity analysis for the cases of single current application (indicated with a broken line) and with post-heat current application (indicated with a solid line).

Figure 8 shows from the temperature histories that the observed HAZ was heated up to the austenite region once and cooled afterwards. The temperature history indicates that the precipitates are produced as a result of autotempering (self tempering during cooling). Autotempering is the annealing or tempering in which carbon is transferred during cooling below the martensite transformation

starting temperature (M_s). In the proximity of M_s , transformed martensite is exposed to a high temperature relatively for a longer time period, and therefore, is prone to further tempering. In general, tempered martensite exhibits higher toughness compared with that of as-quenched martensite.¹⁰⁾ Therefore, in Steel B, fine carbide is precipitated in HAZ by a longer post-heat current application time, thereby improving toughness, and HAZ fractured in the ductility mode like Steel B with a post-heat current application of 0.6 s as shown in Fig. 4, thereby improving CTS.

4.3.2 Mechanism of increase in precipitate of carbide

Next, we examined the reasons for the increase in precipitates in HAZ by a post-heat current application of 0.6 s.

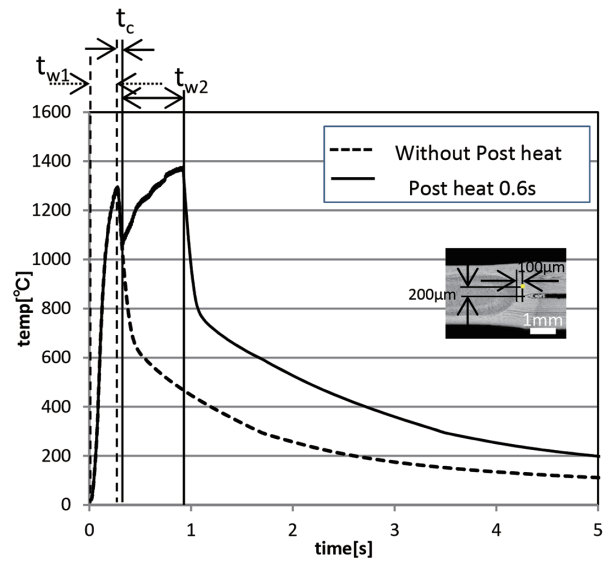


Fig. 8 Estimated temperature histories

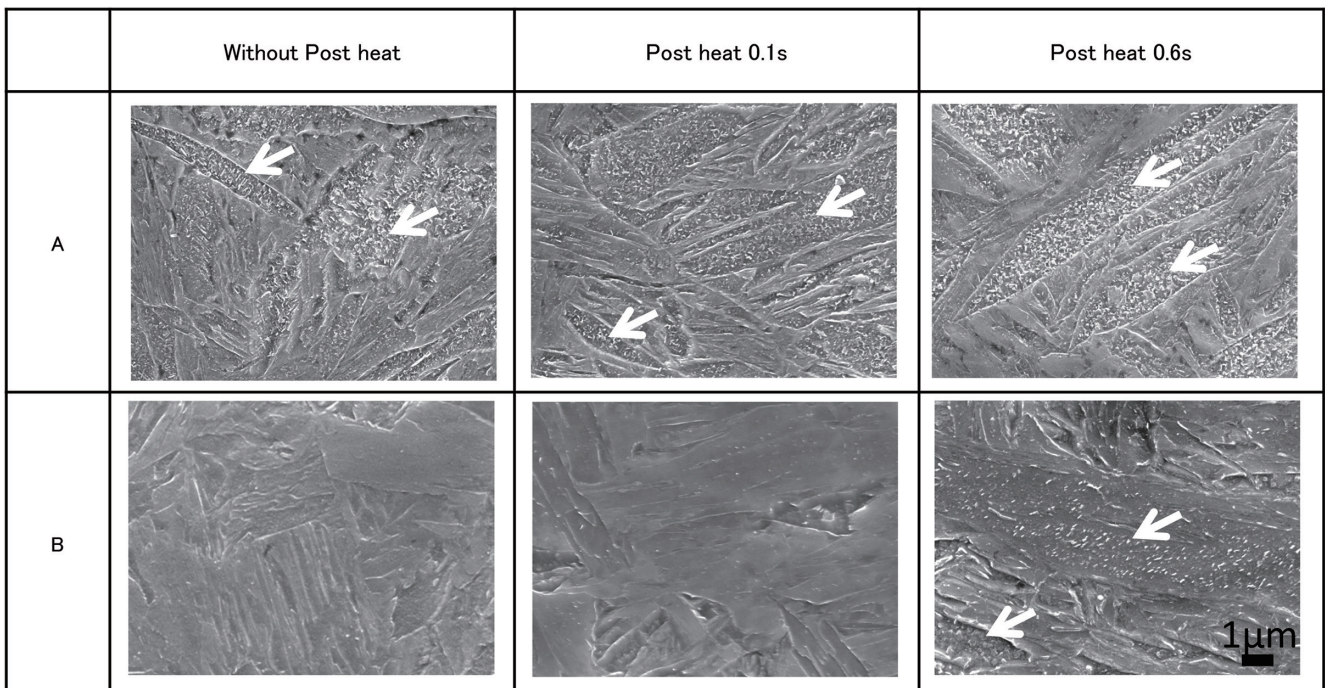


Fig. 7 SEM images of HAZ

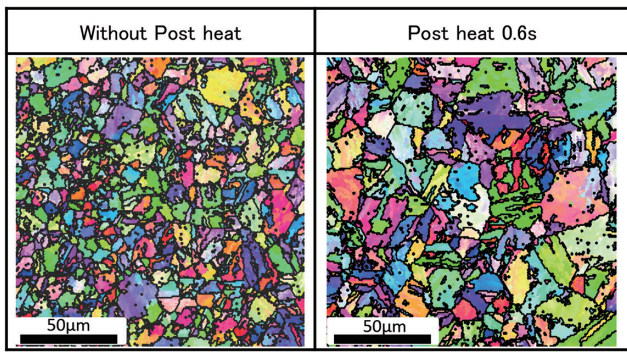


Fig. 9 EBSD IPF image of steel B

The temperature history indicated with a solid line in Fig. 8 is that estimated at the same position as that of HAZ with a post-heat current application of 0.6s shown in Fig. 7, and HAZ stays longer in the single austenite region and the temperature increased significantly by post-heat current application. This indicates that the growth of the grain size of prior austenite increased with post-heat current application. The orientation map of EBSD (Fig. 9) of the final martensite microstructure of HAZ (at the same position as the one in Fig. 7) indicates that the size of the grain observed with the high angle grain boundary (angle: 20°) is larger.

The high angle grain boundary of lath martensite is equivalent to a unit called a block, and it is reported that the wider the block, the larger the grain size of prior austenite.¹²⁾ Accordingly, the prior austenite grain size of HAZ with a post-heat current application of 0.6s became larger than that with single current application. Experimental results by Garcia et al.¹⁴⁾ revealed that in martensite transformation, as the grain size of prior austenite becomes smaller, M_s temperature lowers. Therefore, by elongated post-heat current application time, the HAZ M_s temperature rose, and autotempering more readily progressed, thus precipitating fine carbide.

5. Technique to Reduce Scattering of Weld Joint Strength in Spot Welding of High Tensile Strength Steel Sheets

Shock absorption and securing of driver and passenger space in a cabin at the time of collision are pursued for car bodies. To this end, reliability of the weld joint that joins parts constituting the body is considered crucial. In this regard, the effect of reducing the scattering of weld joint strength by means of segregation alleviation at a nugget edge and the weld-joint-strength improving technique by promoting autotempering of HAZ is proposed.¹⁵⁾ With this effect, reliability of the weld joint in spot welding is considered to increase. The effect of reducing scattering and how such reduction is achieved are shown hereunder.

5.1 Experiment and result thereof

5.1.1 Experiment

The test materials were processed through melting, rolling and annealing on a laboratory base. The sheet thickness was 1.2 mm. C_{eq} , C and P contents of these steels are shown in Table 2. C_{eq} of formula (1) was used.¹²⁾

Table 2 Chemical compositions of sample C (mass%)

	C	Mn	P	C_{eq}
Steel C	0.19	2.6	0.010	0.62

This steel is hereinafter referred to as Steel C. As in the preceding experiment, a servomotor-pressurizing type single phase AC spot welding machine (power frequency 50Hz) was used. Current was applied in two steps as schematically shown in Fig. 1, wherein the main current (I_1) was adjusted so as to form a nugget with a diameter of $5\sqrt{t}$ ($=5.5$ mm), and the post-heat current (I_2) was set at 95% of the main current. Three test levels were set: main current only, post-heat current applications of 0.1 s and 0.3 s. For each of the three test levels, 30 test pieces were prepared and CTS was measured, and then fracture morphology was classified subsequently.

5.1.2 Result of experiment

First, to ascertain the scattering of CTS, histograms with $n=30$ are shown in Fig. 10. In addition, average values and standard deviations (normal distribution) are shown in Table 3.

As a result of the t-test applied to the average values, there was a significant difference between single current application and post-heat current application of 0.1 s, and between single current application and post-heat current application of 0.3 s, with a significance level of less than 1% in either case. Accordingly, improvement in CTS with post-heat current application was recognized. However, in this experiment, no significant difference was observed in the cases of post-heat current application of 0.1 s and 0.3 s. As for scattering, standard deviations based on the assumption of normal distribution show the decrease in scattering in the order of single current application, post-heat current application of 0.1 s and post-heat current application of 0.3s. This suggests that HAZ autotempering promotion has a greater effect on the suppression of scattering of CTS than segregation alleviating post-heat current application.

5.1.3 Examination on scattering

As the relationship between the weld joint strength and the fracture morphology shown in 5.1.2 is suggested as a factor correlating with scattering,¹¹⁾ fracture morphology was investigated. Based on the appearance of samples after the CTS test, the fracture morphology was classified as shown in Table 4 based on Fig. 11. In general, plug fracture and matrix fracture are jointly classified as plug fracture; however, in this classification, they are separately classified.

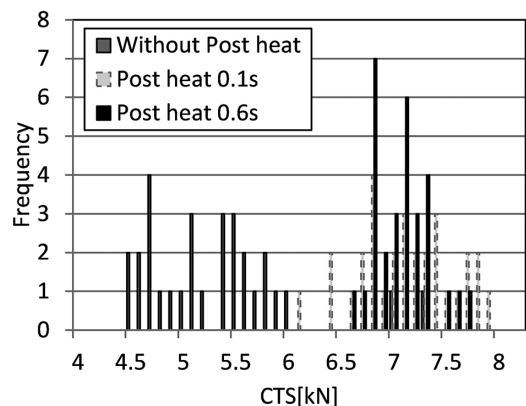


Fig. 10 Histogram of CTS with varied current patterns

Table 3 Average and standard deviation of CTS

	Without post heat	Post heat 0.1 s	Post heat 0.3 s
Average [kN]	5.3	7.1	6.9
Standard deviation [kN]	0.7	0.5	0.3

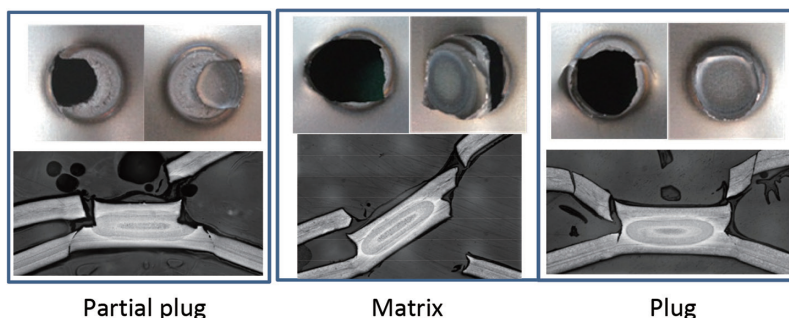


Fig. 11 Classification of fracture morphology

Table 4 Classification of fracture morphology after CTS measurement

	Partial plug	Matrix	Plug
Without post heat	30	—	—
Post heat 0.1 s	8	18	4
Post heat 0.3 s	—	7	28

In single current application, all exhibit partial plug fracture, and with the post-heat current application of 0.1 s, partial plug fracture, plug fracture and matrix fracture are intermingled; with the post-heat current application of 0.3 s, plug fracture and matrix fracture are mixed together. First scattering of CTS is reduced by applying post-heat current to single current application that produces partial plug fracture. The reason for this is that in the partial plug fracture morphology, crack propagation routes are not uniform, and therefore, the maximum loads also fluctuate. Accordingly, partial plug fracture is suppressed by applying post-heat current and the crack propagation routes are arranged relatively uniformly, and scattering is considered to be suppressed thereby. Furthermore, with a longer post-heat current application time, improvement in toughness in HAZ where cracks propagate was achieved, and matrix fracture could be reduced as compared with the case of short term post-heat current application. It is considered that crack propagated in a more stable manner.

6. Conclusion

As technologies for improving weld joint strength and reducing scattering thereof in the spot welding of high tensile strength steel sheets, post-heat current application in a relatively short period of

time to alleviate segregation at the nugget edge, and technologies promoting autotempering of HAZ by applying post-heat current of a relatively long period of time were introduced. One of the advantages of spot welding is its short welding time. The introduced technologies are achievable without causing substantial increase in general spot welding time. Accordingly, they are expected to exert no substantial adverse influence on the production of automobiles, and therefore, they are expected to be beneficial in expanding the application of high tensile strength steel sheets.

References

- 1) Ministry of Land, Infrastructure, Transport and Tourism HP: <http://www.mlit.go.jp/jidosha/kankyo.html>
- 2) Oikawa, H. et al.: Shinnittetsu Giho. (385), 36 (2006)
- 3) WES 7301 Recommended Practice for Spot Welding (Low Carbon Steel and Low Alloy Steel). 1986
- 4) Watanabe, F. et al.: Mathematical Modeling of Weld Phenomena. 10, 653–667 (2013)
- 5) Furusako, S. et al.: Shinnittetsu Giho. (393), 69 (2012)
- 6) Sawanishi, C. et al.: Science and Technology of Welding and Joining. 19 (1), 52 (2014)
- 7) Wakabayashi, C.: Welding Technology. March Issue, (2017)
- 8) Takahashi, M: Tetsu-to-Hagané. 100 (1), 82 (2014)
- 9) Zackay, F. et al.: Transactions of the ASM. (60), 252 (1967)
- 10) Krauss, G.: Materials Science & Eng. A. (273), 40 (1999)
- 11) Matsuyam, K. et al.: Fundamentals and Practice of Resistance Welding. 1st ed. Tokyo, Sanpo Publications Inc., 2011, 242p
- 12) Ginzburg et al.: Flat Rolling Fundamentals. CRC Press, 2000, p. 141
- 13) Furusako, S. et al.: Quarterly Journal of the Japan Welding Society. 33 (2), 160 (2015)
- 14) Garcia-Junceda, A. et al.: Scripta Materialia. (58), 134 (2008)
- 15) Wakabayashi, C.: Preprints of the National Meeting of JWS. 100, 28 (2017)



Chisato WAKABAYASHI
Senior Researcher, Dr. Eng.
Welding & Joining Research Lab.
Steel Research Laboratories
20-1 Shintomi, Futtsu City, Chiba Pref. 293-8511



Seiji FURUSAKO
Senior Researcher, Dr. Eng.
Welding & Joining Research Lab.
Steel Research Laboratories



Yasunobu MIYAZAKI
Chief Researcher, Dr. Eng.
Welding & Joining Research Lab.
Steel Research Laboratories



Fuminori WATANABE
Researcher
Nagoya R & D Lab.